URSI - RCRS 2022, IIT (Indore), India, 1 - 4 December, 2022

Ionospheric disturbances during X1.5 class solar flare of 3 July 2021

S S Rao*(1), and Monti Chakraborty(2)
(1) Udaipur Solar Observatory, Physical Research Laboratory Udaipur 313001, India
E-mail: ssraophy116@gmail.com
(2) Departmentof Electronics and Communication Engineering, Tripura University, Agartala 799022, India
E-mail: montichakraborty@tripurauniv.in

Abstract

An X1.5 solar flare occurred from solar active region 12838 at 1418 UT on 3 July 2021 and its X ray intensity peaked up at ~1429 UT. Besides its location at limb side i.e. ~ 24ºN, 88ºW, it had strong effects in the ionosphere. GPS observations reveal an increase of TEC with 15-30 minutes delay. A shortwave radio blackout (R3 - Strong Radio Blackout) over the Atlantic Ocean has also been observed during this flare that sustained for an hour after the flare peak time.

1. Introduction

Solar flares are the massive solar explosive phenomena through which various wavelengths from radio waves to gamma rays and energetic particles over a few minutes to hours are emitted. Solar flare has its impacts on the ionosphere by increasing ionospheric conductivity/ electron density and resultantly it causes the absorption of radio waves. Various aspects of solar flare impacts on ionosphere like its central meridian distance, (CMD) effects [1], time delay in ionospheric response during flare peak and recovery time, solar zenith angle dependency [2] and Short Wave Radio fadeout, SWF [3] are of topics of concern and need to study each solar flare event.

2. Data Set

The 1-min averaged X ray flux data shown in Fig. 2 are provided by the Space Weather Prediction Center (SWPC) of National Oceanic and Atmospheric administration (NOAA). TEC global maps have been retrieved using the TEC data obtained from the Crustal Dynamic Data Information System's website- https://cdaweb.gsfc.nasa.gov/cgi-bin/eval2.cgi. D-Region Absorption Prediction data and plots are available at SWPC, NOAA- https://www.ngdc.noaa.gov/stp/drap/data. The ionograms (not shown in the paper) for a given station have been obtained from the Global Ionosphere Radio Observatory (GIRO) - https://giro.uml.edu/didbase.

3. Results and Discussions

Solar Monitor's flare prediction system's probabilities are calculated using NOAA Space Weather Prediction Center data. The Sun Watcher using Active Pixel system detector and Image Processing (SWAP) onboard the Project for On Board Autonomy-2 (PROBA2) spacecraft provides images of the solar corona in EUV channel centered at 174 Å as shown in Fig. 1. The positions of the active regions in Fig.1 (left panel) are given in both heliographic and heliocentric co-ordinates. The SDO images 10 different wavelengths measured in angstroms (Å) with its Atmospheric Imaging Assembly (AIA) instrument. The SDO/AIA spectroheliograph of flaring region in spectral EUV channel of 131 Å is emitted by iron-20 (Fe XX) and iron-23 (Fe XXIII) at temperatures greater than 10,000,000 Kelvin, representing the material in flares. The images are typically colorized in teal (right panel of Fig. 1; https://sdo.gsfc.nasa.gov/). The first X class solar flare of solar cycle-25 occurred on July 3, 2021 at 1418 UT from the solar active region 12838. From the same solar active region, two M class solar flare also erupted; first one was M2.7 solar flare at 0704 UT and M1.0 at 1659 UT (Fig. 2). Additionally, three C-class flares were presented from the same active region prior to X class flare on 3 July. It can be seen from Fig. 2 that the first peak in X-ray flux is ~0717 UT which is corresponding to peaking time of M2.7 solar flare on 3 July. Thereafter, a second peak in both XRS A and B is seen ~ 1429 UT, and it decayed at ~1434 UT. This sharp and largest peak on 3 July was corresponding to X1.5 solar flare.

The solar EUV irradiance changes greatly due to the transient solar flares; resulting in corresponding changes in the electron density, temperature, and composition of the thermosphere and ionosphere. The solar X-ray increases the ionospheric conductivity, thus an increase in ionospheric plasma density up to the low-altitude D region owing to solar X-ray emission causes the absorption of radio waves, especially in high-frequency (HF) ranges. This process is called short-wave fadeout (SWF) or the Dellinger effect [3] The Space Weather Prediction Center (SWPC) has designed a model namely D Region Absorption Prediction, D-RAP2,

(https://www.ngdc.noaa.gov/stp/drap/data/) to predict the ionospheric absorption in the D region. The product gives graphical details of high-frequency (HF) radio propagation conditions globally. It can be seen from Fig. 3 that the HF absorption (≥1dB) observed over the Atlantic Ocean during the X1.5 class solar flare of 3 July 2021. A careful look on Figure 3, shows that the HF absorption was nearly 0 MHz before the flare occurrence (~1418 UT) and maximum absorption (35 MHz) seen flare peak time ~(1430 UT). It can also be seen that the HF absorption decreases with the declining phase of the flare. Initially the lower HF up to 5 dB signal was attenuated after the flare beginning. During the flare peak time (~1430 UT) and up to 1439 UT, the 1 dB signal in frequencies range of 30-35 MHz highly attenuated and signal with magnitude > 5 dB was attenuated in lower HF frequencies range of 0-10 MHz. Thus the 1 dB HF signal was high for about 10 minutes just after flare peak time. The normal HF propagation retained after 1600 UT and thus it can be stated that the SWF sustained for more than an hour over the Atlantic region. These results are consistent with the [4]; that the signal absorption increases suddenly and sharply with a sudden increase solar X-ray flux and then recovers over about half an hour following a gradual decrease in solar X-ray flux. The physics behind the ionospheric radio fadeout could be understood as follows; the electrons accelerated by the electric field component of the propagating radio waves collide with the atmospheric constituents. The absorbed energy of the electrons would reradiate without the existence of a neutral atmosphere. However, the electrons lose their energy due to the collisions with neutral particles, which cause a reduction of their reemitted signal. Since the atmospheric density, the collision frequency, and the recombination rate also alter with height, the efficiency of the radio wave absorption in the ionosphere extremely changes with altitude. The electron collision frequency is high in the D-region (2×10^6 s^{-1}) and the HF radio waves below 10 MHz can be intensely attenuated in this region [5]. Therefore, total radio fadeout lasting for tens of minutes or hours can be caused by the enhancement of electron density yielded by level up of electromagnetic radiation or energetic particles during the solar flare of class greater than M.

Another direct ionospheric response to X class solar flare is seen on the ionograms (https://lgdc.uml.edu/common/DIDBFastStationList). We have checked the ionogrmas (not shown here) available at Digital Ionogram Database of Global Ionosphere Radio Observatory (GIRO) for stations located in Atlantic region and found the disappearance of the ionosonde traces ~1430-1435 UT caused by the enhanced ionospheric absorption. We have also checked the lowest recorded ionosonde echo, the minimum frequency (fmin) over ROME (41.80ºN, 12.50ºE), Athens (38ºN, 23.50ºE), Chilton (51.50ºN, 359.40ºE), Juliusruh (54.60ºN, 13.40ºE) and observed the increasing/decreasing trend of fmin before/after the peaking of X1.5 flare and the total blackout coincided with the peak in the X-ray flux. Therefore, the SWF caused by the flare event had a maximum during peaking time.

The EUV measurements by SDO (not shown here) illustrate a strong impact for wavelength order ~30 nm primarily ionizing the F region. Resultantly, it's impact on GNSS measurements. In order to understand the differences in the ionospheric TEC due to the direct flare impact, we give a global map of difference TEC of flare day (3 July 2021) and pre-flare day (2 July 2021) for comparison in Fig. 4.

It becomes perceptible from the global maps of TEC that the extra radiation of the X1.5 flare had an impulsive gain in TEC after the flare peak time. Solar flares induced additional ionization effects more in the D and E regions due to associated enhanced X-ray flux, which has higher penetration depth in the Earth's upper atmosphere. When we look at SF-related changes in difference TEC, the effective change is expected to be small. It is because TEC has maximum contribution from F region. Thus the change observed in TEC on flare day compare to pre-flare day is a maximum of up to 5 TECU. Also, the flare caused increases in TEC is observed to be delayed by ~ 15-30 minutes (See Fig. 4, panel at time 1445 UT and 1500 UT). The delayed TEC response during the flare peak time and the decay time is well explained in the paper by [2] and [6], respectively. The solar flare induced extra ionospheric ionization impacts on GNSS based navigation and the positioning accuracy. Particularly, the increased EUV fluxes cause an immediate increase of the TEC leading to loss of lock in GNSS signal. Also the single and dual frequency precise point positioning is strongly affected during the flare event [7].

4. Summary

The key results observed from present study are summarized in the following.

1. The ionospheric plasma density enhancement during the solar flare causes the absorption of high-frequency (HF) radio waves. This phenomenon is called short-wave fadeout (SWF) which have adverse effect on operation of radio wave communication. For the 3 July 2021 event, the HF absorption (≥1dB) has been observed over the Atlantic Ocean during the X1.5 class solar flare. A maximum absorption (30-35 MHz) during the flare peak time (1429 UT) has been recorded for about 10 minutes, and it decreases with the decaying phase of the flare. The HF propagation re-operated after 1600 UT. Thus, the SWF sustained for more than an hour over the Atlantic region. The SWF is also verified from GIRO ionograms at stations Rome, Athens, Chilton, and Juliusruh wherein the temporal variations in f_{min} shows the disappearance of the echo signal around the fare peak time.
2. Ionospheric TEC was enhanced, reaching its peak during 15-30 minutes after the X1.5 solar flare peak (1429 UT). The delayed TEC response to solar flare during peak and recovery phase of solar flare may be related to disperse ionospheric condition, the dominant recombination processes and thermosphere-

ionosphere coupling, respectively. The changes in TEC during the solar flare indirectly affect the GNSS positioning estimation.

5. Figures

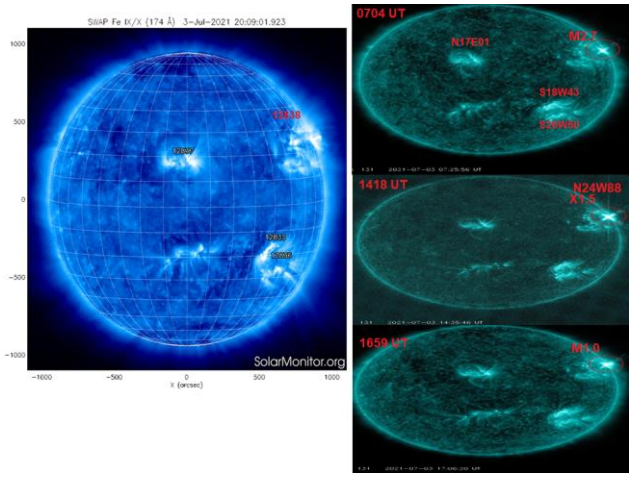

Figure 1. The images of the solar corona in EUV channel centered at 174 Å is shown. The positions of the active regions are given in both heliographic and heliocentric co-ordinates. The solar active regions namely 12835, 12836 and 12837, 12838 on 3 July 2021 are indicated. An X1.5 solar flare occurred from solar active region 12838 (24ºN, 88ºW) on 3 July 2021 is shown in right middle panel.

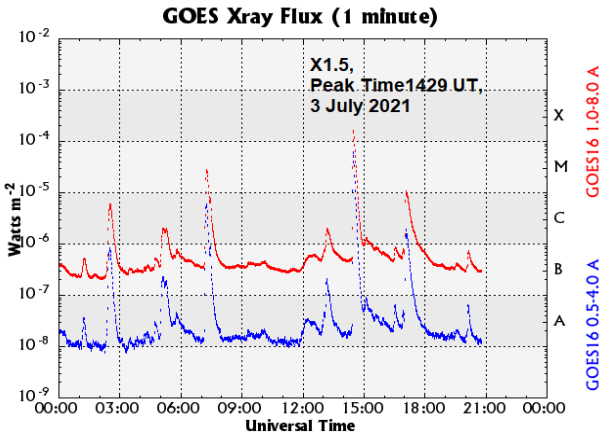

Figure 2. The temporal variation of X ray flux on 3 July 2021 is shown.

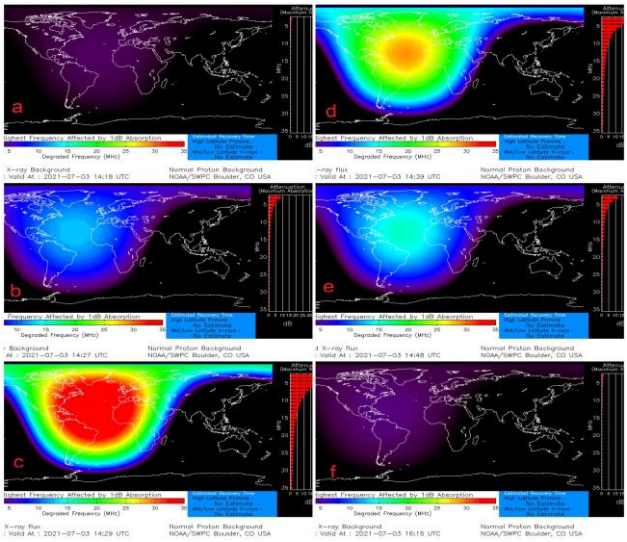

Figure 3. The graphical presentation of high-frequency (HF) radio propagation obtained from the D Region Absorption Prediction, D-RAP2 model is shown.

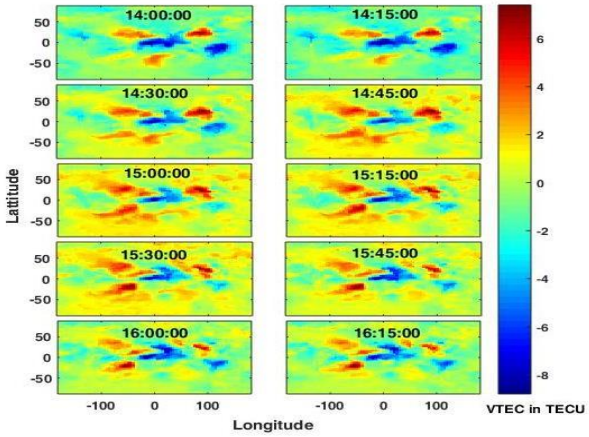

Figure 4. The IGS derived global map of difference TEC of flare and pre-flare day is shown for F region response to X1.5 class solar flare.

6. Acknowledgements

This work is sponsored by CSIR-New Delhi under Pool Scientist Scheme awarded to Dr. S S Rao vide CSIR letter no. B12792 dated 8 July 2021 and File number 13(9203-A) 2021-POOL.

7. References

1. L. Qian, W. Wang, A. G. Burns, P. C. Chamberlin, A. Coster, S.-R. Zhang, & S.C. Solomon, “Solar flare and geomagnetic storm effects on the thermosphere and ionosphere during 6–11 September 2017.” Journal of Geophysical Research: Space Physics, 124, 2019, 2298–2311, doi:.org/ 10.1029/2018JA02617

2. M. Chakraborty, A.K. Singh, S.S. Rao,"Solar flares and geomagnetic storms of September 2017: Their impacts on the TEC over 75°E longitude sector,"Adv. Spce Res.,68(4), 2021,pp. 1825-1835, doi.org/10.1016/j.asr.2021.04.012.

3. J. H. Dellinger, "Sudden disturbances of the ionosphere." J Appl Phys, 8: 1937, 732–751, doi.org/10.1063/1.1710251.

4. S. Chakraborty, J. M. Ruohoniemi, J. B. H. Baker N. Nishitani. "Characterization of short-wave fadeout seen in daytime SuperDARN ground scatter observations." Radio Sci 53: 2018, 472–484. doi.org/10.1002/2017RS006488

5. B. Zolesi, and L. Cander, "Ionospheric Prediction and Forecasting, Springer Geophysics," Springer Heidelberg New York Dordrecht London, 38430-1, 2014, 33–43. doi.org/10.1007/978-3-642.

6. A. Singh, S. S. Rao, V.S. Rathore, *et al.* "Effect of intense solar flares on TEC variation at low-latitude station Varanasi." *J Astrophys Astron* 41, (19) 2020, 1-14, https://doi.org/10.1007/s12036-020-09637-8.

7. J Berdermann, M. Kriegel, D. Bany´s, F. Heymann,M. M. Hoque,V. Wilken, et al. (2018). "Ionospheric response tothe X9.3 Flare on 6 September 2017and its implication for navigation services over Europe," SpaceWeather,16, 2018, 1604–1615. doi.org/10.1029/2018SW001933